

Available online at www.sciencedirect.com

SciVerse ScienceDirect

Nuclear Medicine and Biology xx (2011) xxx–xxx

NUCLEAR
MEDICINE
— AND —
BIOLOGY

www.elsevier.com/locate/nucmedbio

Measuring diffuse metabolic activity on FDG-PET/CT: new method for evaluating Langerhans cell histiocytosis activity in pulmonary parenchyma[☆]

Petr Szturz^{a,*}, Zdeněk Řehák^b, Renata Koukalová^b, Zdeněk Adam^a, Marta Krejčí^a,
Luděk Pour^a, Lenka Zahradová^a, Jiří Vaníček^c, Tomáš Nebeský^d, Roman Hájek^a, Jiří Mayer^a

^aDepartment of Internal Medicine–Hematology, Faculty of Medicine of Masaryk University and University Hospital Brno, Czech Republic

^bDepartment of Nuclear Medicine, PET Centre at the Masaryk Memorial Cancer Institute, Brno, Czech Republic

^cDepartment of Imaging Methods, Faculty of Medicine of Masaryk University and St. Anne's University Hospital Brno, Czech Republic

^dRadiological Clinic, Faculty of Medicine of Masaryk University and University Hospital Brno, Czech Republic

Received 6 June 2011; received in revised form 23 August 2011; accepted 4 October 2011

Abstract

Introduction: Pulmonary Langerhans cell histiocytosis (PLCH) is a rare cause of interstitial lung disease characterized by formation of nodules in the active phase of the disease that evolve into nonactive cystic lesions later on. To evaluate PLCH activity in patients, we developed a new method for measuring diffuse metabolic activity on fluorine-18-fluorodeoxyglucose positron emission tomography/computed tomography (FDG-PET/CT) using a lung-to-liver activity ratio.

Material and Methods: We retrospectively studied a series of 4 FDG-PET and 23 FDG-PET/CT scans from 7 patients with PLCH and analyzed a sample of 100 randomly chosen FDG-PET/CT studies free from any known lung or hepatic diseases. Maximum standardized uptake value (SUVmax) in a spherical volume (6–8 cm in diameter) in the right lung was put into relation with SUVmax in a spherical volume (9–10 cm in diameter) in the reference liver parenchyma to set up the SUVmaxPULMO/SUVmaxHEPAR index. The index values were compared to the disease course in each patient.

Results: In patients with PLCH, a close correlation between the index value and the disease course was found in all seven subjects, where the increasing index values indicated disease activity, while decreasing index values were observed after therapy administration. In the group of 100 healthy control subjects, we found index values lower than 0.3 in 80% and lower than 0.4 in 96% [range: 0.14–0.43; 0.24±0.07 (100)].

Conclusion: Measuring SUVmaxPULMO/SUVmaxHEPAR values and their time-trend monitoring represent simple, noninvasive screening tools allowing an early diagnosis and treatment response follow-up assessment in patients with PLCH.

© 2011 Published by Elsevier Inc.

Keywords: Langerhans cell histiocytosis; Interstitial lung disease; Positron emission tomography; Pulmonary function tests; High-resolution computed tomography (HRCT)

1. Introduction

Pulmonary Langerhans cell histiocytosis (PLCH) is a rare condition, the symptoms of which are nonspecific and

include cough, chest pains and dyspnea, and sometimes, even pneumothorax may be its first manifestation. In the early stages of the disease, small nodules evolving through cavitated forms into thick-walled, later thin-walled and eventually confluent cysts, and start to build up in pulmonary parenchyma. These changes predominantly affect upper lung zones with relative sparing of the lung bases [1]. Radiological appearance of advanced PLCH on conventional radiographs or even high-resolution computed tomography (HRCT) scans may be difficult to distinguish from emphysema, which often leads to delays in getting the

[☆] Conflict of interest: The authors declare that they have no conflict of interest.

* Corresponding author. Department of Internal Medicine–Hematology, University Hospital Brno, Jihlavská 20, 625 00 Brno, Czech Republic. Tel.: +42 0532233064; fax: +42 0532233603.

E-mail address: petr.szturz@fnbrno.cz (P. Szturz).

right diagnosis and initiating proper treatment. In addition, X-ray findings are sometimes inconclusive without any correlation to serious clinical symptoms (Fig. 1).

Langerhans cell histiocytosis limited only to pulmonary parenchyma is a smoke-related interstitial lung disease referred to as isolated PLCH, and it has a better prognosis than Langerhans cell histiocytosis with multisystemic involvement including lungs. Although having different prognoses and therapeutic approaches, these two entities present the same clinical, radiological and histopathological manifestations [2,3]. PLCH is responsible for 3%–5.5% of interstitial lung diseases [4–6]. Larger epidemiologic data are available from Japan [7], where the estimated crude prevalences in males and females are 0.27 and 0.07 per 100,000 population, respectively. Most patients with PLCH are young cigarette smokers between 20 and 40 years of age [1].

Diagnostics include surgical lung biopsy and bronchoalveolar lavage with CD1a+ elements (Langerhans cells) analysis [8]. Additionally, in the setting of multisystemic Langerhans cell histiocytosis, characteristic HRCT scan findings in the lungs may be sufficient for the diagnosis. Treatment is indicated in patients with multisystem involvement or when a progression of pulmonary lesions has been

confirmed. The progression is characterized by increasing numbers of nodules, whereas formation and enlargement of cysts are only a natural disease development into its terminal, end-stage phase. HRCT scans and pulmonary function tests are routinely applied in the follow-up; however, determining the number of nodules on HRCT scans is extremely difficult and time consuming, and pulmonary function tests cannot always distinguish between end-stage cystic disease and active PLCH [6,9].

To facilitate the PLCH activity assessment, we developed and verified a new method for measuring diffuse metabolic activity on fluorine-18-fluorodeoxyglucose (FDG) positron emission tomography/computed tomography (PET/CT) scan imaging using the SUVmaxPULMO/SUVmaxHEPAR index. In this paper, we describe this methodology and verify its validity on a retrospective study of a PLCH patient cohort.

2. Materials and methods

2.1. Patients

During a 21-year period from November 1, 1989, to January 1, 2011, 23 patients were diagnosed with Langerhans

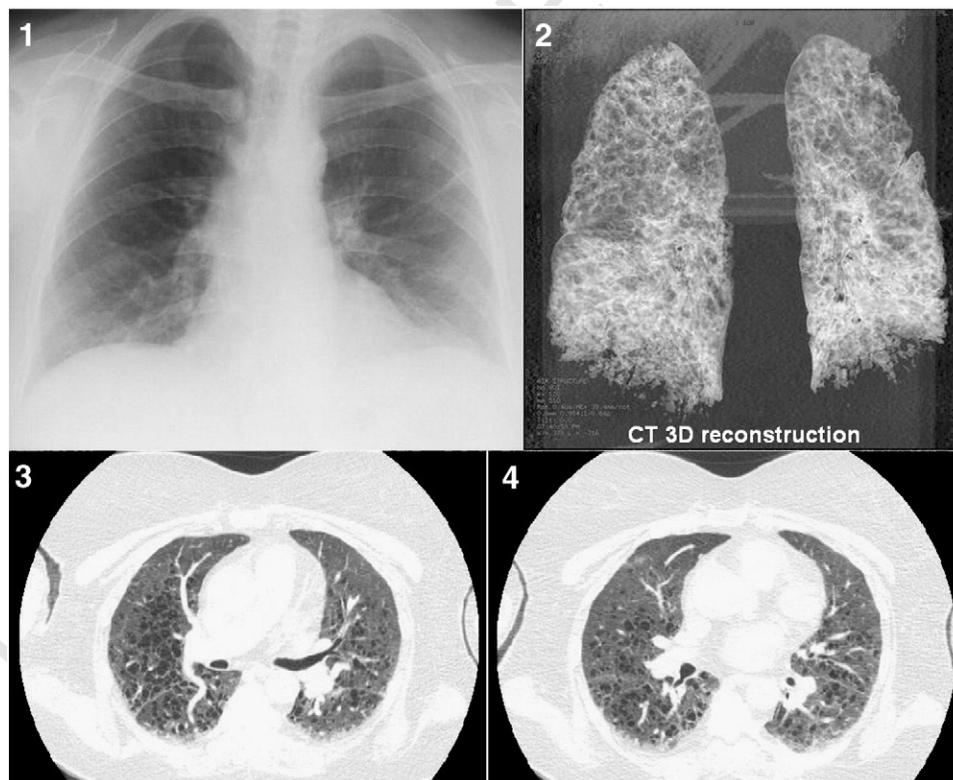


Fig. 1. Different radiological imaging modalities of the chest in a patient with multisystemic Langerhans cell histiocytosis with pulmonary involvement (female, born 1955). The patient presenting with fevers and dyspnea was admitted to hospital with suspected pneumonia in July 2010. There were no abnormalities seen on conventional radiography (1), in contrast to HRCT imaging (3 and 4) showing apart from hypostatic pneumonia also diffuse small cysts (4–15 mm in size) in both lung fields resembling emphysema, which was visualized using 3D reconstruction (2). Cystic lung disease, complicated by bacterial infection, was an accidental finding in this patient. However, retrospective analysis of the SUVmaxPULMO/SUVmaxHEPAR index in preceding four PET examinations (2004–2010) shows a high probability of a previous history of PLCH (Table 2).

cell histiocytosis and followed up at our department. Out of them, 15 patients had either single-systemic (nine patients) or multisystemic (six patients) disease without pulmonary involvement. The remaining eight patients were diagnosed with PLCH, of whom seven underwent FDG-PET scan imaging. In total, 4 FDG-PET and 23 FDG-PET/CT studies were performed between the years 2004 and 2010. The study follow-up period started with the first FDG-PET examination in March 2004.

The indications for FDG-PET or FDG-PET/CT scanning included: (a) searching for multiorgan involvement of an extrapulmonary (verified by bone, lymph node or skin biopsies) Langerhans cell histiocytosis (four scans) as well as (b) of known PLCH (two scans), (c) differential diagnosis of pituitary stalk infiltration (one scan) and (d) follow-up of patients (20 scans). The patients were free from any other active lung or liver disease at the time of PET scanning. The diagnosis of PLCH was based on pathological examinations (three patients) or pathognomonic HRCT scan findings (four patients). Patients who did not agree to the use of their medical records for research were not included in this study.

2.2. FDG-PET/CT scan imaging

In the PLCH patient cohort, we performed FDG-PET and FDG-PET/CT scanning in euglycemia after fasting for 6 h. FDG-PET scan images of the body, at the extent from the proximal thirds of femurs to the cranial base (with included

the head in four scans), were obtained 60 min after intravenous injection of fluorodeoxyglucose (range of applied activity: 312–409 MBq). Until 2008, data acquisition was performed on a PET scanner (ECAT ACCEL SIEMENS) in a three-dimensional (3D) mode and, later, from 2008, on a hybrid PET/CT scanner (True Point PET-CT Biograph 64 SIEMENS). Emission and transmission scans were reconstructed by using an iterative reconstruction algorithm. On acquired data, attenuation correction was applied. Due to repeated follow-up FDG-PET/CT scanning, in most studies, low-dose CT protocol reducing radiation load significantly was used. With the remaining studies, high-dose CT mode was applied. The scan field of view was 50 or 70 cm according to a patient's body habitus. The acquisition parameters for CT were as follows: slice 5 mm, collimation 24×1.2 mm, pitch 0.8 mm. To optimize lung parenchyma imaging, the following reconstruction algorithm was used: slice 1.5–2.0 mm, kernel B 80 f (ultra sharp), reconstruction increment 0.4 mm, window–lung. Maximum standardized uptake values (SUVmax) were measured for semiquantitative analysis.

2.3. SUVmaxPULMO/SUVmaxHEPAR index

Nodules in PLCH often measure several millimeters (4–6 mm) and are below detectable levels of used PET scanners (about 7 mm), which precludes direct measurement of their activity. Therefore, we tried to find these active lesions in a

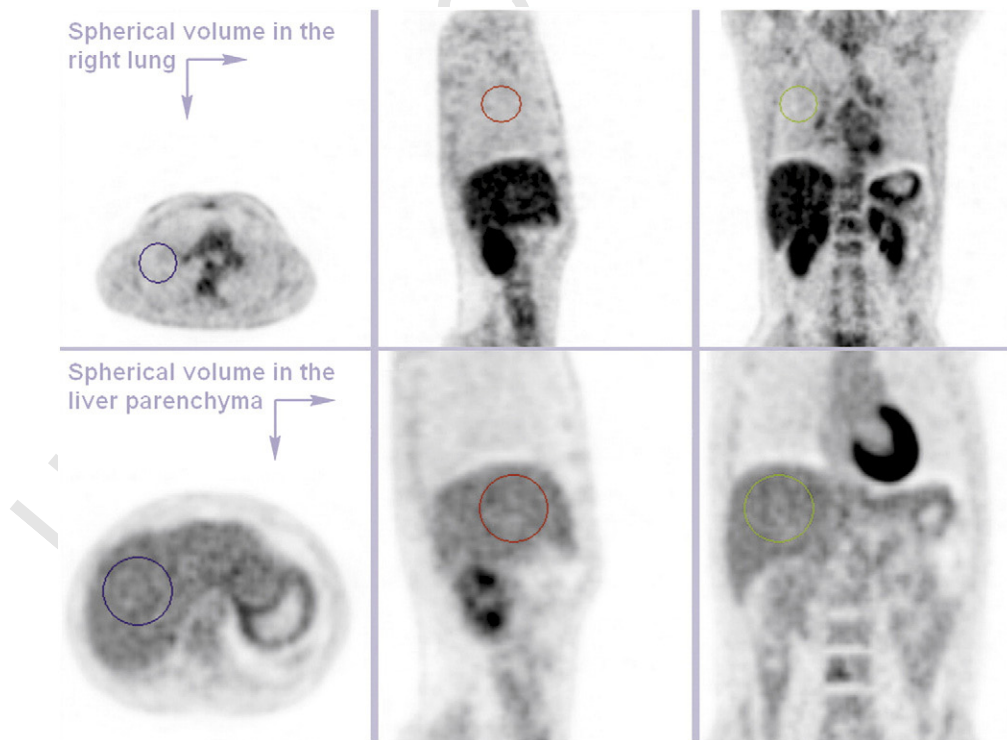


Fig. 2. SUVmax in a spherical volume (6–8 cm in diameter) in the right lung was put into relation with SUVmax in a spherical volume (9–10 cm in diameter) in the reference liver parenchyma to set up the SUVmaxPULMO/SUVmaxHEPAR index. Considering the topographical differences between the lungs and the liver, we were more limited in demarcating the volume of interest in the lung parenchyma, which therefore has smaller diameter.

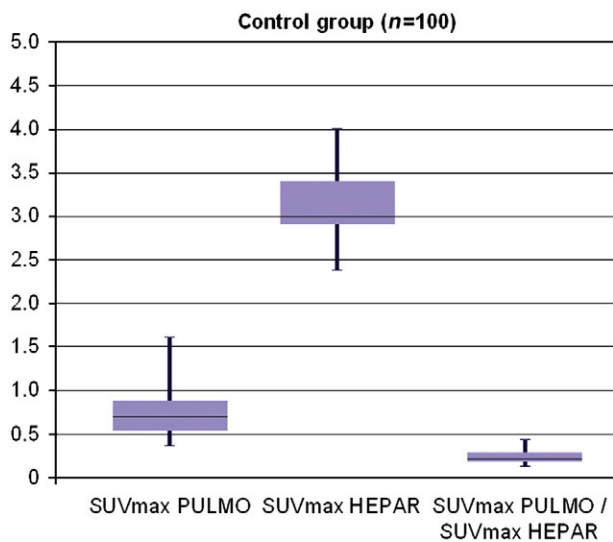


Fig. 3. Box plot of SUV data of control group: median SUV_{max}PULMO=0.70 [range: 0.380–1.600; 0.74±0.26 (100)], median SUV_{max}HEPAR=3.00 [range: 2.40–4.00; 3.11±0.35 (100)], median SUV_{max}PULMO/SUV_{max}HEPAR=0.22 [range: 0.14–0.43; 0.24±0.07 (100)].

larger area. Considering the anatomical conditions, we chose the volume of interest shaped into spheres of 6–8 cm in diameter in the right lung. The metabolic activity was measured in the right upper and middle lung fields. These are the regions of predominant PLCH involvement. The right side without heart and pericardium is more suitable for demarcating the volume of interest and requires only the exclusion of the hilar structures and pleura, where the activity can be increased physiologically. Moreover, in the lower lung fields, numerous motion artifacts are common. This selection of size and location of the volume of interest strives to maximize the probability of occurrence of the majority of active lesions in the most anatomically suitable region while preserving an easy way of determination in a daily routine.

To decrease the variability between single examinations as well as to compare examinations from different scanners, lung-to-liver activity ratio was assessed. In the liver parenchyma, we chose volume of interest shaped into spheres of 9–10 cm in diameter following analogous principles as in the lungs (Fig. 2). Consequently, SUV_{max} in the right lung and SUV_{max} in the reference hepatic

parenchyma were measured, and their relationship expressed as the SUV_{max}PULMO/SUV_{max}HEPAR index was determined and used for PLCH activity evaluation.

In our analysis of a sample of 100 randomly chosen FDG-PET/CT studies free from any known lung or hepatic diseases, either oncological or nononcological, we found index values lower than 0.3 in 80% and lower than 0.4 in 96% [range: 0.14–0.43; 0.24±0.07 (100)]. No index values higher than 0.5 were identified in the healthy population. The range of applied activity was 302–425 MBq [354.51±32.12 (100)], and that of blood glucose levels was 3.1–8.1 mmol/L [5.00±1.09 (100)]. Further SUV data are summarized in Fig. 3.

3. Results

Six males, all with a history of smoking, and one female, 31 to 48 years of age at the time of first FDG-PET scanning [39.7±6.5 (7)], were included in this study. The mean follow-up period was 17 months [range: 9–79 months; 30.4±29.0 (7)]. Six patients had a multisystemic Langerhans cell histiocytosis with pulmonary involvement and received at least one line of therapy. One patient had isolated PLCH, and this patient has not been treated yet. In patients with multisystemic disease, the following organs were affected: lungs (100%), skin (65%), bones (50%), brain (30%), ear (30%) and lymph nodes (15%). Respiratory symptoms (dyspnea, cough) were present in five patients (71%), of whom one patient suffered from recurrent pneumothorax. Demographic and clinical data are shown in Tables 1 and 2.

All patients underwent FDG-PET scan imaging (4 PET scans and 23 PET/CT scans). The acquired data, summarized in Table 3, were correlated to the clinical course of the disease, HRCT findings, pulmonary function tests and pathological examinations. In total, 18 HRCT studies [2.6±1.3 (7)] and 13 pulmonary function tests [1.9±1.5 (7)] were performed in seven patients. We have found a close correlation between the SUV_{max}PULMO/SUV_{max}HEPAR index values and the above-mentioned disease activity parameters (Table 2). Consequently, we worked with two variables, the index value and the metabolic tumor activity, and found a relationship with positive slope, i.e., increasing index value corresponds with increasing metabolic tumor

t1.1 Table 1

t1.2 Main demographic and clinical characteristics of seven patients with PLCH

t1.3	Date of birth, sex	Smoking habitus	Disease onset (years)	Extrapulmonary involvement	Diagnosis of pulmonary involvement (years)
t1.4	1972, M	Smoker	21	Bones	34
t1.5	1974, M	Smoker	33	Skin, brain (pituitary stalk), ear	34
t1.6	1969, M	Ex-smoker	39	Skin	40
t1.7	1963, M	Active and passive smoker	43	Ear	45
t1.8	1973, M	Smoker	34	Skin, bones, lymph nodes	35
t1.9	1963, M	Smoker	45	Isolated PLCH	45
t1.10	1955, F	Nonsmoker	22	Skin, bones, brain, ear	54

t2.1 Table 2

t2.2 Correlation between the SUVmaxPULMO/SUVmaxHEPAR index and disease course in seven patients with PLCH

t2.3	Date of birth, sex	Date of PET-CT ^a	SUVmax PULMO/SUVmax HEPAR	Disease course and symptoms of pulmonary involvement	Interpretation of SUVmaxPULMO/SUVmaxHEPAR index in relation to disease course
t2.4	1972, M	Mar 04	0.44	After 5 cycles of cladribine therapy, remission of bone lesions	High index value due to active smoking
t2.5		Jan 05	0.45	Lasting remission of bone lesions	
t2.6		Feb 07	0.51	Dyspnea, cough	Progression of PLCH
t2.7		Jun 08	0.47	Smoking cessation leading to relief of symptoms	Gradual remission of PLCH in accordance with relief of symptoms after cessation of smoking
t2.8		Jan 09	0.29		
t2.9		Feb 10	0.27		
t2.10	1974, M	Mar 09	0.21	Screening admission PET/CT	
t2.11		Feb 10	0.27	Progression of pituitary stalk infiltration on brain MRI; therapy initiation	Increased index value suggests progression in lungs
t2.12		Jun 10	0.22	Regression of pituitary stalk infiltration after 3 cycles with cladribine	Therapy effective also in PLCH as suggested by decreasing index value
t2.13	1969, M	May 09	0.57	Disease activity (recurrent pneumothorax, 3 times); therapy initiation	High index value confirms PLCH
t2.14		Mar 10	0.22	After 6 cycles of cladribine therapy, partial remission of skin lesions	Therapy effective in PLCH as suggested by decreasing index value
t2.15	1963, M	Mar 09	0.57	Screening admission PET/CT	High index value confirms PLCH
t2.16		Aug 09	0.53	After 4 cycles of cladribine therapy	Gradual remission of PLCH after successful cladribine therapy
t2.17		Mar 10	0.38	Follow-up PET/CT	
t2.18	1973, M	Jan 09	0.54	Screening admission PET/CT; dyspnea, cough	High index value confirms PLCH
t2.19		Jun 09	0.31	After 4 cycles with cladribine therapy	Therapy effective also in PLCH
t2.20		Nov 09	0.36	1st relapse (confirmed by lymph node and skin biopsies); cough	Increased index value suggests relapse in lungs
t2.21		Jan 10	0.27	After 2 cycles of salvage chemotherapy CHOEP; relief of symptoms	Remission of PLCH after chemotherapy
t2.22		Jul 10	0.28	4 months after autologous transplantation	Lasting remission of PLCH after autologous transplantation
t2.23		Oct 10	0.48	2nd relapse (confirmed by lymph node biopsy)	Increased index value suggests 2nd relapse in lungs
t2.24	1963, M	Jul 08	0.21	Screening admission PET/CT; intermittent cough	
t2.25		Feb 10	0.24	Stable disease not requiring therapy; lasting intermittent cough	Slightly increased index value in patient with stable clinical manifestation, but still continuing his smoking habitus
t2.26	1955, F	Mar 04	0.42	Screening admission PET/CT; slight effort dyspnea	High index value suggests pulmonary involvement
t2.27		Jan 09	0.31	After several cycles with vinblastine, prednisone and etoposide	Therapy effective also in PLCH
t2.28		Mar 10	0.14	Progression in brain; therapy initiation	Further remission of PLCH
t2.29		May 10	0.17	After 2 cycles with cladribine	Lasting remission of PLCH
t2.30		Oct 10	0.38	Further progression in brain, chemoresistant disease	Increased index suggests progression of PLCH

t2.31 CHOEP, cyclophosphamide+doxorubicin+vincristine+etoposide+prednisone.

t2.32 ^a Between 2004 and 2007, only PET scans were made.

205 activity and vice versa. The increasing trends of index
 206 values were seen in five patients, where they indicated
 207 PLCH activity (i.e., pulmonary symptoms, formation of
 208 nodules on HRCT or abnormal pulmonary function tests),
 209 whereas decreasing trends of index values were observed in
 210 six patients after therapy administration, signaling reduced
 211 metabolic tumor activity. Furthermore, in four patients,
 212 SUVmaxPULMO/SUVmaxHEPAR index values higher
 213 than 0.5 proved to be diagnostic for pulmonary involve-
 214 ment, demonstrating its role as a strong positive predictive
 215 marker. Fig. 4 shows the disease course with corresponding
 216 index values in one patient (male, born 1973).

217 Quantitative analysis of HRCT findings in patients with
 218 PLCH, consisting of assessment of the exact count of

219 nodules and cystic formations, is almost impossible to be
 220 obtained. Therefore, the PET-CT findings were correlated to
 221 a semiquantitative radiological evaluation of HRCT scans,
 222 and neither sensitivity, specificity, accuracy nor predictive
 223 values can be exactly calculated in our study.

4. Discussion 224

225 The clinical course of PLCH is very divergent and
 226 impossible to be predicted for an individual patient [2,3].
 227 About 50% of patients with isolated PLCH have a favorable
 228 prognosis with total disease remission, i.e., reduction of
 229 pulmonary nodules either spontaneously or after corticoid

t3.1 Table 3

t3.2 An overview of PET-CT data in 7 patients with PLCH

t3.3	Date of birth, Sex	Date of PET-CT ^a	Applied activity (MBq)	Blood glucose levels (mmol/L)	SUVmax PULMO	SUVmax HEPAR	SUVmax PULMO / SUVmax HEPAR
t3.4	1972, M	Mar-04	327	4.4	0.80	1.83	0.44
t3.5		Jan-05	321	5.8	0.81	1.79	0.45
t3.6		Feb-07	335	4.1	1.02	2.01	0.51
t3.7		Jun-08	337	4.8	1.06	2.24	0.47
t3.8		Jan-09	315	5.2	0.92	3.22	0.29
t3.9		Feb-10	352	4.7	0.89	3.25	0.27
t3.10	1974, M	Mar-09	414	4.6	0.93	4.39	0.21
t3.11		Feb-10	431	4.8	0.89	3.25	0.27
t3.12		Jun-10	466	5.4	0.78	3.53	0.22
t3.13	1969, M	May-09	377	4.7	1.88	3.30	0.57
t3.14		Mar-10	393	5.2	0.78	3.53	0.22
t3.15	1963, M	Mar-09	372	4.7	1.78	3.11	0.57
t3.16		Aug-09	421	4.9	1.79	3.36	0.53
t3.17		Mar-10	401	4.7	1.03	2.71	0.38
t3.18	1973, M	Jan-09	330	6.3	1.34	2.49	0.54
t3.19		Jun-09	336	5.6	0.68	2.23	0.31
t3.20		Nov-09	330	5.3	1.18	3.24	0.36
t3.21		Jan-10	338	5.7	0.88	3.30	0.27
t3.22		Jul-10	317	5.5	0.75	2.72	0.28
t3.23		Oct-10	292	6.4	1.40	2.98	0.48
t3.24	1963, M	Jul-08	338	4.7	0.69	3.30	0.21
t3.25		Feb-10	354	5.1	0.95	3.96	0.24
t3.26	1955, F	Mar-04	344	4.4	1.02	2.45	0.42
t3.27		Jan-09	337	5.8	1.00	3.19	0.31
t3.28		Mar-10	357	6.7	0.48	3.49	0.14
t3.29		May-10	351	5.4	0.53	3.15	0.17
t3.30		Oct-10	386	7.0	1.45	3.8	0.38

t3.31 ^a Between 2004–2007 only PET scans were made.

therapy. Cessation of smoking proved to be essential in therapy management, leading to remission in many cases described [6,10,11]. Nevertheless, cystic lung damage is irreversible. Moreover, PLCH implies a higher risk of lung cancer, especially in smokers, and a higher risk of other malignancies as well [12].

The greatest challenge is the evaluation of PLCH disease activity and, consequently, therapy effectiveness. In recent years, based on a contrasting rate of glucose utilization between rapidly proliferating tumor cells and surrounding normal tissue, much attention has been devoted to the benefit of FDG-PET and FDG-PET/CT scan imaging for determining the extent of Langerhans cell histiocytosis and therapy response evaluation.

Derenzini et al. [13] used FDG-PET for evaluating the effectiveness of MACOP-B chemotherapy in four patients. The FDG-PET scan was able to detect additional lesions missed by other modalities in two patients. A negative interim FDG-PET predicted a long-lasting remission in three of four patients. Phillips et al. [14] published the same experience as they compared the benefit of FDG-PET/CT to bone scans, CT, magnetic resonance imaging (MRI) and conventional radiography for determining the extent of Langerhans cell histiocytosis and evaluation of therapy response in 44 patients (41 children and 3 adults). They

concluded that whole-body FDG-PET scans can detect disease activity and early response to therapy with greater accuracy than other imaging modalities in patients with Langerhans cell histiocytosis affecting bones and soft tissues. Furthermore, FDG-PET is also beneficial for an early diagnosis of neurodegenerative Langerhans cell histiocytosis [15].

However, a MEDLINE literature search revealed only one paper evaluating FDG-PET scan imaging in PLCH, the work from authors Krajicek et al. [16], who described their cohort study with 11 patients. PET-scan-positive patients had predominantly nodular lung disease with more than 100 nodules usually under 8 mm in size, whereas PET-scan-negative patients had predominantly cystic lung disease with nodules numbering less than 25 in a field of examination.

In our study, all pathology in the lung parenchyma was below detectable levels of the PET scanner (less than 7 mm), and we did not find large active lesions. Notwithstanding the observations of Krajicek et al., we describe a new methodology for diffuse metabolic activity evaluation of the lung parenchyma and present the possibility to objectify the results by comparing them with the simultaneously measured activity of the reference liver parenchyma. The evaluation of pulmonary activity based on the index, the ratio of the measured SUVmax value in a spherical volume of the

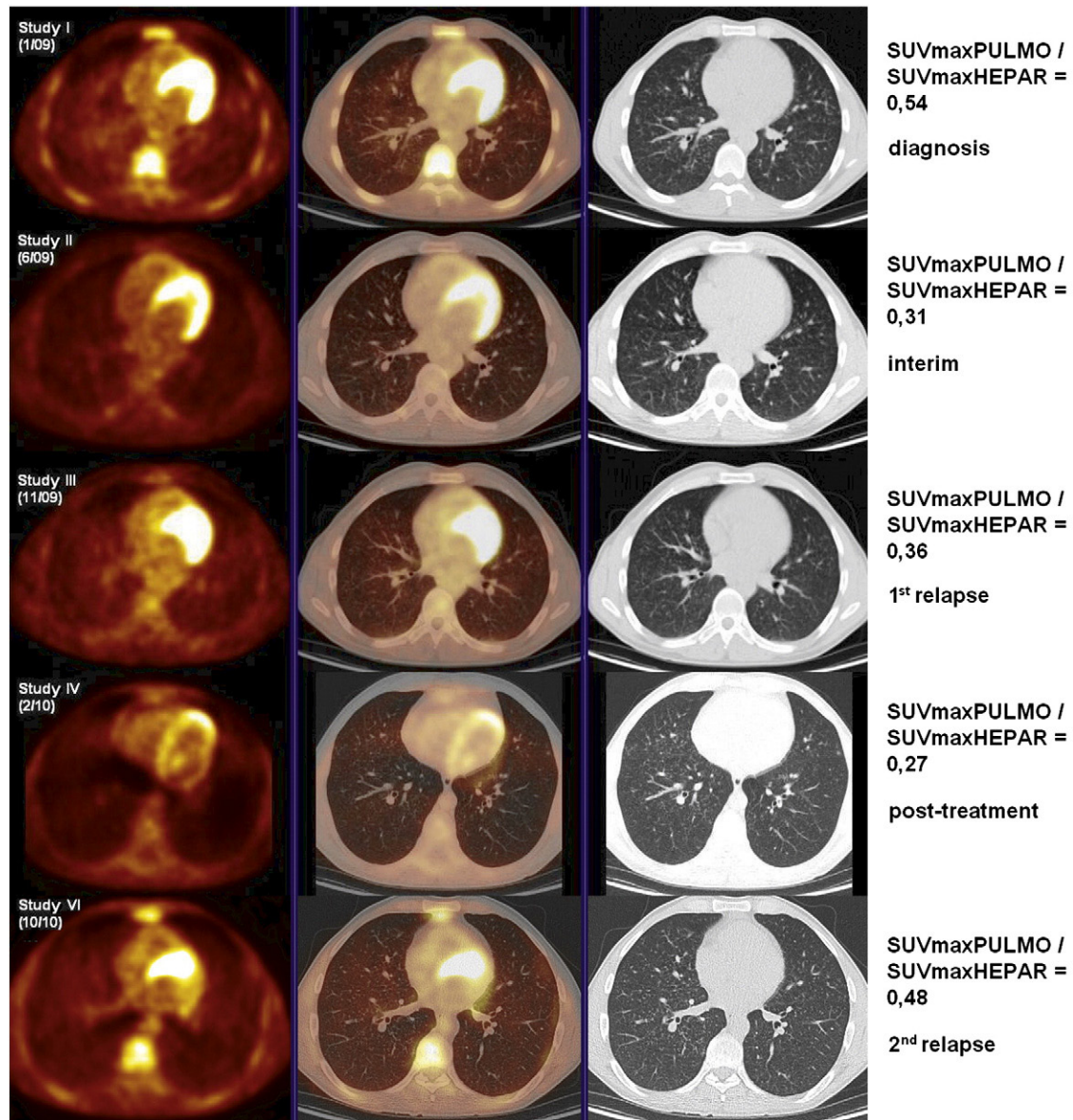


Fig. 4. Series of FDG-PET/CT images of a patient with multisystemic Langerhans cell histiocytosis with pulmonary involvement (male, born 1973). High index value on admission PET/CT together with pathognomonic HRCT finding (multiple small nodules with sporadic cysts) and clinical symptoms (dyspnea, cough) was diagnostic for PLCH. Interim PET/CT after two cycles with cladribine shows a therapy response which correlated with regression of lymphadenopathy and relief of the symptoms, including perianal pruritus and B-symptoms (night sweats, fever and weight loss). However, an aggressive form of Langerhans cell histiocytosis with recurrent relapses was the case. The index value corresponded closely with the disease course. We consider myocardial FDG uptake to be physiological.

280 right lung to the measured SUVmax value in a spherical
 281 volume of the liver — the SUVmaxPULMO/SUVmaxHE-
 282 PAR index — which we propose and which we have
 283 verified, has not been published so far. We are aware of the
 284 fact that the method we used is not common and, with such
 285 small lesions, it is negatively biased by the partial-volume
 286 effect characterized by increasing underestimation of SUV
 287 with decreasing lesion sizes [17]. The index may be
 288 influenced by concomitant factors affecting either lungs or
 289 liver (e.g., other interstitial lung diseases, benign tumors,
 290 active infections or noninfectious inflammations, cholesta-
 291 sis, cirrhosis). Moreover, hyperinsulinemia [18], higher

glucose level [19] and advanced age [20] were found to be
 related to increased FDG uptake by liver. 293

Currently, except for HRCT of the lungs and pulmonary
 function tests, there is no other modality that informs more
 accurately on PLCH activity. Traditional FDG-PET scan
 imaging is not possible due to the small size of nodules
 which cannot be reliably resolved by the PET scanner.
 Therefore, we consider the measuring and long-term
 monitoring of the index SUVmaxPULMO/SUVmaxHEPAR
 to be very useful additional tools for PLCH activity
 evaluation. Based on our analysis of a sample of 100
 randomly chosen PET/CT scans, as mentioned above, and on

304 this retrospective study, we found that SUV_{max}PULMO/
 305 SUV_{max}HEPAR index values higher than 0.5 bear high
 306 probability of pulmonary involvement in patients with
 307 Langerhans cell histiocytosis.

308 In conclusion, measuring the SUV_{max}PULMO/SUV-
 309 maxHEPAR index and its time-trend monitoring represent
 310 simple noninvasive screening tools for PLCH, allowing us to
 311 optimize the therapeutic management in the patients. An
 312 early diagnosis of pulmonary involvement with a prompt
 313 initiation of therapy may prevent progressive cystic damage
 314 to the lungs. The index measurement also enables an
 315 effective monitoring of therapy response and follow-up of
 316 patients with PLCH.


317 Acknowledgment

318 This work was supported in part by the IGA
 319 of The Ministry of Health (NT11154, NS10387,
 320 FUNDIN MZ0MOU2005); The Ministry of Education,
 321 Youth and Sports (LC06027, MSM0021622434); and
 322 MUNI/A/1012/2009.

323 References

- 324 [1] Vassallo R, Ryu JH. Pulmonary Langerhans' cell histiocytosis. Clin
 325 Chest Med 2004;25(3):561–71.
- 326 [2] Tazi A. Adult pulmonary Langerhans' cell histiocytosis. Eur Respir J
 327 2006;27(6):1272–85.
- 328 [3] Sundar KM, Gosselin MV, Chung HL, Cahill BC. Pulmonary
 329 Langerhans cell histiocytosis: emerging concepts in pathobiology,
 330 radiology, and clinical evolution of disease. Chest 2003;123
 331 (5):1673–83.
- 332 [4] Thomeer M, Demedts M, Vandeurzen K, VRGT Working Group on
 333 Interstitial Lung Diseases. Registration of interstitial lung diseases by
 334 20 centres of respiratory medicine in Flanders. Acta Clin Belg 2001;
 335 56(3):163–72.
- 336 [5] Gaensler EA, Carrington CB. Open biopsy for chronic diffuse
 337 infiltrative lung disease: clinical, roentgenographic, and physiological
 338 correlations in 502 patients. Ann Thorac Surg 1980;30(5):411–26.
- 339 [6] Colby TV, Lombard C. Histiocytosis X in the lung. Hum Pathol 1983;
 340 14(10):847–56.
- [7] Watanabe R, Tatsumi K, Hashimoto S, Tamakoshi A, Kuriyama T, 341
 Respiratory Failure Research Group of Japan. Clinico-epidemiological 342
 features of pulmonary histiocytosis X. Intern Med 2001;40 343
 (10):998–1003. 344
- [8] Vassallo R, Ryu JH, Colby TV, Hartman T, Limper AH. Pulmonary 345
 Langerhans'-cell histiocytosis. N Engl J Med 2000;342(26): 346
 1969–78. 347
- [9] Schönfeld N, Frank W, Wenig S, Uhrmeister P, Allica E, Preussler H, 348
 et al. Clinical and radiologic features, lung function and therapeutic 349
 results in pulmonary histiocytosis X. Respiration 1993;60(1):38–44. 350
- [10] Mogulkoc N, Veral A, Bishop PW, Bayindir U, Pickering CA, Egan JJ. 351
 Pulmonary Langerhans' cell histiocytosis: radiologic resolution 352
 following smoking cessation. Chest 1999;115(5):1452–5. 353
- [11] Friedman PJ, Liebow AA, Sokoloff J. Eosinophilic granuloma of 354
 lung. Clinical aspects of primary histiocytosis in the adult. Medicine 355
 (Baltimore) 1981;60(6):385–96. 356
- [12] Tomaszefski JF, Khiyami A, Kleinerman J. Neoplasms associated 357
 with pulmonary eosinophilic granuloma. Arch Pathol Lab Med 1991;115 358
 (5):499–506. 359
- [13] Derenzini E, Fina MP, Stefoni V, Pellegrini C, Venturini F, Broccoli 360
 A, et al. MACOP-B regimen in the treatment of adult Langerhans cell 361
 histiocytosis: experience on seven patients. Ann Oncol 2010;21 362
 (6):1173–8. 363
- [14] Phillips M, Allen C, Gerson P, McClain K. Comparison of FDG-PET 364
 scans to conventional radiography and bone scans in management of 365
 Langerhans cell histiocytosis. Pediatr Blood Cancer 2009;52 366
 (1):97–101. 367
- [15] Ribeiro MJ, Idbaih A, Thomas C, Remy P, Martin-Duverneuil N, 368
 Samson Y, et al. 18F-FDG PET in neurodegenerative Langerhans cell 369
 histiocytosis : results and potential interest for an early diagnosis of the 370
 disease. J Neurol 2008;255(4):575–80. 371
- [16] Krajicek BJ, Ryu JH, Hartman TE, Lowe VJ, Vassallo R. Abnormal 372
 fluorodeoxyglucose PET in pulmonary Langerhans cell histiocytosis. 373
 Chest 2009;135(6):1542–9. 374
- [17] Hoetjes NJ, van Velden FH, Hoekstra OS, Hoekstra CJ, Krak NC, 375
 Lammertsma AA, et al. Partial volume correction strategies for 376
 quantitative FDG PET in oncology. Eur J Nucl Med Mol Imaging 377
 2010;37(9):1679–87. 378
- [18] Iozzo P, Geisler F, Oikonen V, Mäki M, Takala T, Solin O, et al. 18F- 379
 FDG PET Study. Insulin stimulates liver glucose uptake in humans: an 380
 18F-FDG PET Study. J Nucl Med 2003;44(5):682–9. 381
- [19] Kubota K, Watanabe H, Murata Y, Yukihiko M, Ito K, Morooka M, 382
 et al. Effects of blood glucose level on FDG uptake by liver: a FDG- 383
 PET/CT study. Nucl Med Biol 2011;38(3):347–51. 384
- [20] Lin CY, Ding HJ, Lin CC, Chen CC, Sun SS, Kao CH. Impact of 385
 age on FDG uptake in the liver on PET scan. Clin Imaging 2010; 386
 34(5):348–50. 387
 388
 389

AUTHOR QUERY FORM

 ELSEVIER	Journal: NMB Article Number: 7094	Please e-mail or fax your responses and any corrections to: Shayna Bayard E-mail: sbayard@verizon.net Tel: 215-844-8326 Fax: 215-844-4292
--	--	---

Dear Author,

Please check your proof carefully and mark all corrections at the appropriate place in the proof (e.g., by using on-screen annotation in the PDF file) or compile them in a separate list. Note: if you opt to annotate the file with software other than Adobe Reader then please also highlight the appropriate place in the PDF file. To ensure fast publication of your paper please return your corrections within 48 hours.

For correction or revision of any artwork, please consult <http://www.elsevier.com/artworkinstructions>.

Any queries or remarks that have arisen during the processing of your manuscript are listed below and highlighted by flags in the proof. Click on the 'Q' link to go to the location in the proof.

Location in article	Query / Remark: click on the Q link to go Please insert your reply or correction at the corresponding line in the proof
Q1	Please confirm that given names and surnames have been identified correctly.
Q2	Please spell out if an abbreviation/acronym.

Thank you for your assistance.